Fibrin Assembly in Human Plasma and Fibrinogen/Albumin Mixtures

Jim Torbet*

Institut Laue-Langevin, 38042 Grenoble Cedex, France, and Max-Planck-Institut für Festkörperforschung, Hochfeld-magnetlabor, 38042 Grenoble Cedex, France

Received September 19, 1985; Revised Manuscript Received April 18, 1986

ABSTRACT: Magnetic birefringence is used to monitor the kinetics of thrombin-catalyzed fibrin polymerization in model systems of increasing complexity (i.e., fibrinogen solutions, fibrinogen/albumin mixtures, and plasma anticoagulated with citrate) and in plasma containing free calcium which is the physiological condition. The introduction of albumin into fibrinogen solutions shortens the lag period and enhances fiber thickness. The polymerization progress curves are sigmoidal at zero or low albumin concentrations, but at physiological and higher concentrations, they become hyperbola-like from the end of the lag period. High albumin concentration has thus induced a change in the assembly kinetics. The progress curves from plasma in which the cascade is dormant are also hyperbola-like although they round off more quickly because of antithrombin activity. In plasma containing free calcium, thrombin is endogenously produced, and the progress curves are nearly linear; hence, the assembly kinetics are very different from those of the model systems. The curves are not influenced by calcium-dependent cross-linking involving factor XIIIa. The progress curves are also linear when polymerization is induced with Russell's viper venom, which by directly activating factor X circumvents earlier steps in the cascade. This implies that linear polymerization is caused by events posterior to factor X activation and are thus likely to be largely dependent on the functioning of the prothrombinase complex. Addition of thrombin to plasma containing free calcium reduces the lag period. At low exogenous thrombin levels, the polymerization rate is increased, and the progress curves remain linear. However, at higher levels, the curves become more complicated and, paradoxically, full polymerization takes longer. This paper shows how the mechanisms in control of thrombin activity regulate fibrin formation differently depending on the conditions. Fiber thickness and gel morphology vary considerably with the conditions of formation. It is emphasized that simple model systems can give a misleading representation of clotting behavior in more physiological conditions.

Hemostasis involves the vascular wall, platelets, and a number of plasma proteins and cofactors. The complex cascade of reactions leading to clot formation (Jackson & Nemerson, 1980; Nemerson & Furie, 1980) culminates in the transformation of the soluble plasma protein fibrinogen, after thrombin activation, into a polymeric fibrin network. Polymerization has been elucidated in aqueous buffer systems using principally electron microscopy, light-scattering, and gel filtration techniques. The structure of fibrinogen and its conversion into fibrin have recently been reviewed (Hermans & McDonagh, 1982; Doolittle, 1984). Fibrinogen is an elongated molecule (length 450 Å) of molecular weight 340 000 and is composed of two identical halves each containing three polypeptide chains, Aα, Bβ, and γ. Thrombin catalyzes the release of the small negatively charged fibrinopeptides A and B. Removal of the former initiates linear polymerization while that of the latter promotes, although is not essential for, lateral aggregation. From experiments mostly involving the addition of thrombin to solutions of purified fibrinogen, fibrin assembly is qualitatively understood as the longitudinal association of monomers into double-stranded protofibrils with a half-monomer stagger; long protofibrils associate laterally to form an interlinked network of fibers. From about the gelation point, the reaction follows pseudo-first-order kinetics, and the fibrin network existing at this point is largely consolidated by fiber lateral growth (Freyssinet et al., 1983). The protofibrils within fibers are in axial register and pack with a degree of three-dimensional regularity (Torbet et al., 1981). The fibers exhibit a long pitch axial twist (Hewat et al., 1983; Müllar et al., 1984) and can form bundles or cables (Buchanan et al., 1977). The diameter of fibers is not uniform and has been described as consisting of a major network of thick fibers together with a minor network of thin fibers (Shah et al., 1982). The junctions between fibers and their frequency of occurrence also form part of this hierarchy of interrelated structural features linking protofibrils, fibers, and the gel network.

A great deal has been gleaned from studies of purified systems, but in physiological conditions there are many additional processes which are likely to have a major bearing on clot assembly and structure. For example, factor XIII binds strongly to fibrinogen (Greenberg & Shuman, 1982; Janus et al., 1983) and after thrombin activation covalently cross-links fibrin in the presence of calcium ions (Folk & Finlayson, 1977). Fibronectin (Mosher, 1976; Chen et al., 1977), α_2-antiplasmin (Sakata & Aoki, 1980; Tamaki & Aoki, 1981), and plasminogen (Rakoczi et al., 1978; Garman & Smith, 1982; Sakata et al., 1984) are all incorporated into fibrin. Also, there are the diverse interactions leading up to the activation of factor X, followed by formation of the prothrombinase complex and thrombin generation (Jackson & Nemerson, 1980; Nemerson & Furie, 1980). The activity of the resulting thrombin can be reduced (Messmore, 1982) and possibly enhanced by plasma proteins (Ganguly et al., 1983).

Here fibrin formation is studied in conditions of increasing physiological relevance ranging from fibrinogen/albumin mixtures to whole human plasma using magnetic orientation. The object of these experiments is to help identify the physiologically important processes that control the kinetics of clot assembly and structure. Magnetic birefringence has been used previously to study the progress of polymerization in purified fibrinogen/fibrin (Torbet et al., 1981; Freyssinet et al., 1983).

* Address correspondence to the author at the Institut Laue–Langevin.

0006-2960/86/0425-5309$01.50/0

It works equally well in circumstances in which by far the majority of the proteins are non clot forming because the relatively large diamagnetic anisotropy of the fibrin fibers leads to selective high orientation. The diamagnetic anisotropy of fibrin constitutes an innate specific label; its use in the present context can be likened to a form of contrast enhancement.

Materials and Methods

Plasma Preparation. Citrated human plasma was obtained by collecting freshly drawn blood (9 volumes) into 3.8% (w/v) sodium citrate (1 volume) followed by centrifugation at $\simeq$5000*g* for 20 min at 15 °C. The final plasma concentration was reduced to 80–85% including the dilutions resulting from the addition of thrombin and calcium. The plasma was usually used within a few hours; otherwise, it was stored below −18 °C and remelted at 37 °C prior to use. Fresh and frozen plasma behaved similarly. Whole undiluted human plasma was obtained by centrifuging fresh blood (without anticoagulant) at 5000*g*, 12 °C, for 15 min. The resulting plasma was kept on melting ice until it was used within a few hours. The results reported are from plasma donated by a single individual. Serum obtained after clotting took place in the presence of free calcium did not show renewed fibrin growth on addition of thrombin, but serum collected in the absence of free calcium ([thrombin] < 0.3 NIH unit mL^{-1}) could be reclotted, showing that all the fibrinogen had not been converted into fibrin. The concentration of fibrinogen in plasma was assayed following the Diagnostica Stago procedure. Bovine thrombin was obtained from the Institut de Sérothérapie Hématopoiétique and stored at −70° C at 20 NIH units mL^{-1}. Experiments were performed by using a stock solution of 5 NIH units mL^{-1} which was further diluted immediately prior to mixing. Human albumin came from Fluka. Factor XIII subunit A concentrate from human placenta was Fibrogammin from Behringweke. The final concentration of added factor XIII ranged from 1 to 2 times that present in normal plasma, and it was incubated from 0 to 100 min with thrombin (1–2 NIH units mL^{-1}) and sometimes also with up to 20 mM calcium. Russell's viper venom was obtained from Sigma. Fibrinogen was purified from human plasma as described in Kekwick et al. (1955). Unless otherwise stated, the buffer was 0.05 M tris(hydroxymethyl)aminomethane hydrochloride (Tris-HCl) containing 0.1 M NaCl, 0.5 mM ethylenediaminetetraacetic acid (EDTA), and 0.01% (w/v) NaN_3 at pH 7.5. All measurements were made at 37 °C.

Birefringence Measurements. Samples undergoing polymerization were contained in quartz cells with an optical path length of 0.1 cm. This was increased to 1 or 3 cm in order to measure the much weaker birefringence given by nonclotting plasma, serum, and albumin solutions. The cells were placed in a temperature-stabilized (±0.1 °C) sample holder in a Bitter-type magnet which had a small radial bore and could give a maximum field of 13.5 T; 1 T = 10^4 G. The birefringence, $\Delta n(\lambda = 6328$ Å), was measured by using a combined photoelastic modulation and compensation technique which has been described in detail (Maret & Weill, 1983).

Theory. The magnetic orientation of fibrin has been discussed previously (Torbet et al., 1981; Freyssinet et al., 1983). The following quantities are defined: $\Delta n(t)$ = variation with time, t, of the difference in the refractive indexes of light linearly polarized parallel and perpendicular to the applied field direction; $C = C_p(t) + C_M(t)$ = concentration of polymer plus that of monomer; Φ = polymer orientation function which is 0 at random orientation and 1 at full alignment ($0 \leq \Phi \leq 1$); Δn_s = birefringence when the polymer of concentration C is fully aligned, $\Phi = 1$. Following Freyssinet et al. (1983), the birefringence induced when polymerization is carried out in a constant field is related to the polymer concentration by

$$\Delta n(t) = C_p(t)\frac{\Delta n_s}{C}\Phi \qquad (1)$$

This equation is valid provided the background from unpolymerized material is constant or weak and the average optical anisotropy of the polymer does not change during the reaction. These conditions are met during pure fibrin formation (Freyssinet et al., 1983). The background birefringence from plasma and albumin solutions is measured to be both weak and invariant. However, proteins other than fibrin do make up a small proportion of a plasma clot and on binding could alter the average clot optical anisotropy, but this effect is very probably minor as fibrin is both highly anisotropic and by far the major clot component.

The parameter Φ in eq 1 could in principle vary throughout the reaction if the average orientation of the polymers continually improved as they grew. Gelation and polymer entanglement can reduce or eliminate this complication. With pure fibrin, Φ is constant from about the gelation point which occurs at an early stage in the reaction (Freyssinet et al., 1983). In the present study, it has been verified that the variation of Φ during polymerization is not significant by checking that the birefringence curves have the same shape over a range of magnetic field strengths which induce from weak to near saturation in orientation. Figure 3 provides an example. Hence, $\Delta n(t)$ is simply proportional to the polymer concentration, $C_p(t)$, and its shape, wherein the principal information is contained, depends directly on the kinetics of assembly.

The magnitude of the birefringence can give information on the relative average fiber width although it is also a function of the rate of assembly. Slow polymerization will lead to an increase in Φ until assembly is slowed down to the point where there is time available for all the growing polymers to rotate into their equilibrium orientation. Similarly, very fast reactions are difficult to investigate as Φ will remain small because the time scale of orientation is greater than that of the reaction. Thick fibers favor larger Φ than thin because their diamagnetic anisotropy is greater. This is confirmed by studies on the purified system in which calcium addition increases both fiber thickness and the birefringence while at high ionic strength the signal is much reduced and the fibers are thin (Freyssinet et al., 1983). Thus, when the rates of polymerization are similar, the sample giving the largest final birefringence must be composed of the thickest fibers. When the rates are significantly different, the same conclusion applies to the fastest assembling sample if it gives the largest birefringence. However, if the birefringence is largest with slow assembly, conclusions about the relative thickness are more different to make. The magnetic field strength should be less than the value ($\Phi < 1$) that gives complete orientation as otherwise there would be no variation in birefringence due to differing average fiber diameters.

The birefringence, when all the monomers are converted into a polymer, is given by $\Delta n_s\Phi$. In conditions in which complete conversion is not attained, dividing the measured birefringence at the end of the reaction by $\Phi\Delta n_s$ and correcting for differences in Φ give an estimate of the fractional degree of polymerization. This is most conveniently used near full alignment as Φ is then known to be near unity.

Results and Discussion

In most of the experiments described below, fibrinogen is a small fraction of all the proteins present. In plasma, fibrinogen constitutes only 2–5 mg mL^{-1} of the approximately

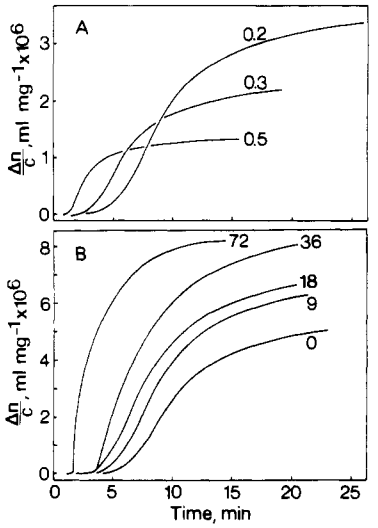

FIGURE 1: Variation of the birefringence normalized to fibrinogen concentration (c = 1 mg mL^{-1}) as fibrin forms at 37 °C in a constant magnetic field of 5.9 T (1 T = 10^4 G). (A) Fibrinogen solution polymerized by the addition of thrombin concentration shown in NIH units per milliliter. (B) Fibrinogen/albumin mixed solutions polymerized by the addition of 0.12 NIH unit mL^{-1} thrombin; albumin concentration is shown in milligrams per milliliter.

80 mg mL^{-1} protein about half of which is albumin. Nonclotting plasma exhibits an interesting donor- and temperature-dependent magnetic birefringence which probably reflects chylomicron behavior (Torbet, 1986). However, the signals from plasma before and after clot formation are similar and also much weaker ($|\Delta n| < 2 \times 10^{-8}$; 37 °C; H = 7 T) than that given by fibrin. Thus, the shape and magnitude of the birefringence curves reported below depend solely on the properties of fibrin.

Fibrin Formation in the Presence of Albumin. As shown previously, when fibrin formation is initiated by adding a rate-limiting amount of thrombin to a solution of fibrinogen in a constant magnetic field, the variation in the induced birefringence is sigmoidal (Figure 1A), and the reaction follows pseudo-first-order kinetics from near the gelation point (Freyssinet et al., 1983). The value of the birefringence increases as the lag period is extended and the rate of assembly is reduced. This is because slow assembly results in improved orientation as the resulting fibers are thicker (Hantgan & Hermans, 1979), and there is more time available for the polymers to rotate under the influence of the field. The addition of albumin to fibrinogen solutions shortens the lag period and increases the birefringence signal (Figure 1B) even though the rate of polymerization is markedly faster. This is reminiscent of the influence calcium has on the birefringence curves (Freyssinet et al., 1983). Thus, albumin, like calcium, both reduces the lag period and increases fiber thickness. At high albumin concentrations (36 and 72 mg mL^{-1}), the onset of fiber formation is more abrupt, and after the end of the lag period, the shape becomes hyperbola-like (Figure 1B), indicating a minor change in the early events of assembly. This has not been observed with calcium.

Quicker release of the fibrinopeptides cannot explain the albumin effect as this would be equivalent to increasing the thrombin concentration in pure fibrinogen solutions which is clearly not true (Figure 1). This is in agreement with Wilf et al. (1985), who also found that in addition to albumin, γ-globulin, hemoglobin, and ovalbumin decrease the lag period. These authors also present evidence indicating that the cocondensation of the added protein with fibrin is unlikely to have a significant effect on assembly. Consequently, they

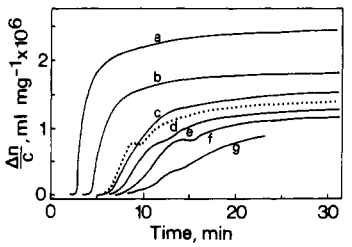

FIGURE 2: Variation of the birefringence normalized to fibrinogen concentration, $\Delta n/c$ (c = 2.4 mg mL^{-1}), as citrate-treated human plasma was clotted at 37 °C in a constant magnetic field of 6.1 T after addition of thrombin to a final concentration in NIH units per milliliter of (a) 0.12, (b) 0.10, (c and d) 0.09, (e) 0.08, (f) 0.075, and (g) 0.07. Measurements were made with other samples up to 0.5 unit mL^{-1} thrombin. The curves had the same shape as (a) and (b), but polymerization was still incomplete. Higher concentrations could not be effectively studied as the delay between mixing and exposure to the field is longer than the lag period.

suggest that the reduction in the lag period is primarily due to nonspecific volume exclusion arising from increased fractional occupancy of solution volume by macromolecules. The additional results reported here (i.e., thickening of fibers with increasing albumin concentration and change in assembly at high albumin concentration) are qualitatively compatible with predicted effects of volume exclusion (Minton, 1981, 1983).

Fibrin Formation in Citrated Plasma. The magnetic birefringence curves recorded after adding different concentrations of thrombin to citrate-treated plasma are shown in Figure 2 (citrate chelates calcium ions, thus inhibiting thrombin formation). The clots of Figure 2 are dilute and mechanically fragile so the modulations in the curves which only occur with low thrombin concentrations and are not accurately reproducible (compare curves c and d, figure 2) probably reflect physical movement of the gel rather than an assembly event. At higher thrombin concentrations, the overall shape is hyperbola-like as observed from fibrinogen/albumin mixtures with a high albumin content (Figure 1B). However, the final birefringence is about 75% smaller even though orientation is high (Figure 6B). This is because the intervention of the endogenous antithrombins (Messmore, 1982), principly antithrombin III, prevents complete polymerization. Their effect becomes more marked as the concentration of thrombin is reduced (Figure 2). The snake venom enzyme reptilase gives rise to progress curves which are very similar in both shape and magnitude when added to citrated plasma or fibrinogen/albumin mixtures (J. Torbet, unpublished results). This enzyme is not significantly inhibited by plasma antithrombins but releases only the A fibrinopeptides. There is thus no evidence to suggest that specific interactions between fibrinogen or fibrin and other plasma proteins with the possible exception of albumin have a significant effect on the kinetics of fibrin assembly in citrate-treated plasma. However, the corollary is not true of the gel structure which is noticeably different (compare panels A and B of Figure 6) in citrated plasma and fibrinogen/albumin mixtures.

Fibrin Formation in Free Calcium Containing Plasma. In normal free calcium containing plasma, thrombin is endogenously generated from prothrombin during the latter phase of the coagulation cascade. The ensuing clot formation was investigated in experiments summarized in Figures 3 and 4 which deal respectively with whole plasma and recalcified citrated plasma. These curves are completely different in character from those given by purified protein (Figure 1) or citrate-treated plasma lacking free calcium (Figure 2). In whole plasma (Figure 3a–c) as in recalcified citrated plasma (Figure 4a), the clot grows rapidly and almost linearly until

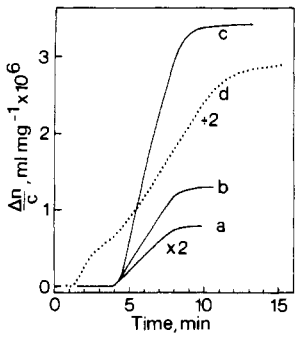

FIGURE 3: Variation with time of the birefringence normalized to fibrinogen concentration, $\Delta n/c$ (c = 4.3 mg mL^{-1}), as whole undiluted human plasma (a–c) was clotted at 37 °C in a magnetic field of (a) 2, (b) 3.5, and (c) 5.9 T. In (d), the field was 5.9 T, and thrombin (0.14 NIH unit mL^{-1}) was added which resulted in a small dilution to c = 4.07 mg mL^{-1}. The final birefringence of curves (a–c) varies linearly with the square of the field, and, therefore, the orientation is far from complete. In fixed conditions, the shapes of the curves a–c are independent of the magnetic field strength, and measurements can be made in 2 T (a) and probably less. The sample optical path length can be increased about 10-fold to 1 cm, with a concomitant increase in signal, before the reduction in transmitted light intensity becomes troublesome. Therefore, magnetic field strengths which are easily and inexpensively attainable are adequate for the study of plasma clot formation.

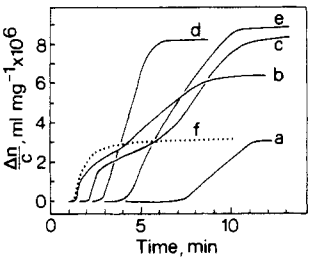

FIGURE 4: Variation of the birefringence normalized to fibrinogen concentration, $\Delta n/c$ (c = 2.1 mg mL^{-1}), as citrated human plasma was clotted at 37 °C in a constant magnetic field of 7.1 T. The added calcium and thrombin concentrations in millimolar and NIH units per milliliter, respectively, were (a) 16, 0; (b) 16, 0.12; (c) 16, 0.10; (d) 16, 0.09; (e) 16, 0.06; and (f) 0, 0.18.

completion is abruptly attained. These assembly kinetics favor a rapidly formed localized clot.

The rate and time distribution of thrombin production must have a bearing on fibrin assembly, but there are known calcium-dependent interactions involving fibrin directly which are potentially of consequence. The last enzyme in the coagulation cascade is the thrombin-activated, calcium-requiring factor XIIIa which by introducing γ-glutamyl-ε-lysine intermolecular bonds stabilizes fibrin (Folk & Finlayson, 1977) and cross-links fibronectin (Mosher, 1976; Chen et al., 1977) and α_2-antiplasmin (Sakata & Aoki, 1980; Tamaki & Aoki, 1981) to the fibrin α-chain. Suggestively, fibronectin is cross-linked at a near linear rate in the purified system (Tamaki & Aoki, 1981). However, citrate-treated plasma that had been passed through a gelatin–agarose column to remove fibronectin (Engvall & Ruoslahti, 1977) gave a set of curves with shapes indistinguishable from those (Figure 4) given by normal citrate-treated plasma. Fibronectin does not therefore significantly influence the kinetics of fibrin assembly. Turning attention to the ligation of fibrin, it was found that the addition of glycinamide, a competing substrate for factor XIIIa (Lorand & Jacobsen, 1962; Gormsen et al., 1967), up to 10 mM made little impact on the clotting behavior of recalcified citrate-treated plasma. Similarly, exogenous factor XIIIa had little affect on the shape of the curves due to fibrin formation either in recalcified citrate-treated plasma or in pure fibrinogen

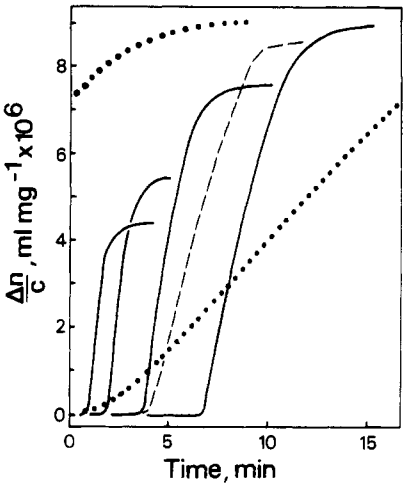

FIGURE 5: Variation of the birefringence normalized to fibrinogen concentration, $\Delta n/c$ (c = 2.2 mg mL^{-1}), as citrated human plasma was clotted at 37 °C with 10 mM added calcium in a constant magnetic field of 6 T. (Dotted lines) Recalcification only; lag period was about 27 min and is not shown. (Solid lines) Concentration of Russell's viper venom added simultaneously with recalcification from left to right in 5 × 10^{-3}, 5 × 10^{-5}, 5 × 10^{-6}, and 1.25 × 10^{-6} mg mL^{-1}. The drop in signal as the concentration is increased is due to a reduction in orientation probably because of the increasing rate of assembly. (Dashed line) 0.1 NIH unit mL^{-1} thrombin was added simultaneously with recalcification.

solutions. Hence, no evidence was obtained to implicate factor XIIIa and associated fibrin-coupled interactions with the linear calcium-dependent phase of clot assembly. This conclusion is not unexpected as in the purified system the rate of release of both fibrinopeptides is not changed by factor XIIIa (Janus et al., 1983). The regulation of assembly is therefore primarily associated with the profile of thrombin activity.

The penultimate step in the process of thrombin formation is the generation of activated factor X (factor Xa) which forms part of the prothrombinase complex that converts prothrombin into thrombin. The coagulant protein from Russell's viper venom specifically activates factor X in the presence of calcium (Furie & Furie, 1976) and in so doing bypasses the preceding steps in the activation cascade. It can therefore be employed to help probe how the physiological processes before and after factor Xa production influence fibrin formation.

Figure 5 shows the birefringence curves obtained from citrated plasma on simultaneous recalcification and addition of Russell's viper venom. The curves, which have the familiar linear form (Figures 3 and 4), are all very similar in shape over the wide range of enzyme concentrations used. The highest enzyme concentration in Figure 5 is 0.005 mg mL^{-1}, but even at saturation levels, up to 200 times higher, the shape was invariant and the lag period was not much further reduced. These curves imply that the near-linear kinetics of fibrin assembly are controlled by events subsequent to factor Xa formation. Thus, the production of thrombin by the prothrombinase complex and the modulation, by plasma proteins, of its activity by inhibition (Messmore, 1982) and possibly by enhancement (Ganguly et al., 1983) lead to near-linear clot growth in conditions that approach physiologic (Figures 3a–c and 4a).

The addition of a small amount of thrombin to recalcified citrated plasma reduces the lag period and accelerates polymerization with little change in the near-linear form of the progress curves (Figure 4d,e). At slightly higher exogenous thrombin concentrations, the lag period is further reduced; however, the overall rate of polymerization is decreased, and the kinetics of assembly are changed (Figure 4b,c). This is

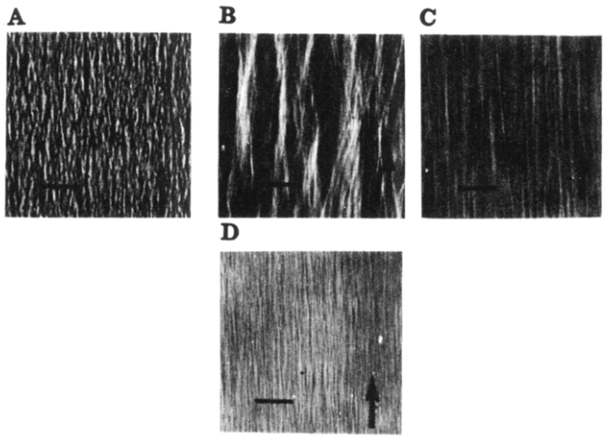

FIGURE 6: Micrographs of oriented clots contained in quartz cells taken with a polarizing microscope immediately after the birefringence measurements without further treatment such as dehydration or fixation. The bar corresponds to 100 μm, and the arrow indicates the field direction. (A) Sample with 70 mg mL^{-1} albumin, 1 mg mL^{-1} fibrinogen, and 0.12 NIH unit mL^{-1} thrombin in Figure 1B. This looks very much like the gels obtained from calcium/fibrinogen solutions. (B) Citrated plasma sample a of Figure 2: 0.12 NIH unit mL^{-1} thrombin, no free calcium. (C) Citrated plasma sample c of Figure 4: added thrombin and calcium concentrations were respectively 0.1 NIH unit mL^{-1} and 16 mM. Some clots prepared in this way had cables that were sufficiently regular in thickness and packing to give rise to a pair of first-order lateral peaks by optical diffraction of the micrographs. (D) Recalcified citrate-treated plasma; gel observed after the completion of the dotted curve in Figure 5. The oriented gels obtained with Russell's viper venom look similar.

also found with whole plasma (Figure 3). The progress curves become bicomposite with a hyperbola-like region followed by a linear phase, the successive features being associated with added thrombin activity, its neutralization by antithrombins, and retarded endogenous thrombin generation. Thus, the response is adapted according to the degree of perturbation. This is possibly achieved in the following way. Thrombin both activates and inactivates factors V and VIII, the cofactors of thrombin and activated factor X production, respectively (Jackson & Nemerson, 1980; Nemerson & Furce, 1980). The increase in the rate of polymerization at low levels of added thrombin (Figure 4d,e) could therefore be due to faster activation of these factors, while the delay in the appearance of the linear growth phase at higher thrombin levels (Figures 4b,c) might be caused by their inhibition.

Gel Structure. A qualitative estimate of the relative diameter of fibers can be inferred from the magnitude of the birefringence curves. The magnitude of the birefringence arising after recalcification (Figure 4a) is much smaller, although polymerization is slower, than that given when thrombin is also added (Figure 4d) while it is similar to that obtained in the absence of free calcium (Figure 4f). However, in the latter condition not only is polymerization quicker but also as discussed above, the concentration of fibrin is much lower. Hence, the average fiber diameter is smallest in the free calcium only condition, but it is increased by exogenous thrombin and surprisingly is largest in the absence of free calcium as only in these samples were individual fibers thick enough to be seen in the light microscope (Figure 6). In the condition nearest physiological, thinner fibers are favored which is the inverse of what would have been expected from studies of model systems. This suggests that endogenous thrombin activation has a dominant influence on gel structure although it cannot be excluded that the possible variable binding of subsidiary clot proteins might be of some import. For example, more plasminogen binds to non-cross-linked than to cross-linked fibrin (Rakoczi et al., 1978; Sakata et al., 1984), and it can alter fibrin structure at least in purified systems (Garman & Smith, 1982). However, the studies reported above on the influence of factor XIIIa cross-linking interactions on clot assembly furnished no evidence to suggest that they could significantly modify fiber thickness. It should also be borne in mind that the behavior of free calcium containing plasma is likely to be altered in situ due to interactions with other components and surfaces such as platelets (Dhall et al., 1983) and the vascular wall.

The oriented clots are highly polymorphic; the fibers are not distributed uniformly but are rather grouped into cables with characteristics depending on the conditions of formation (Figure 6). Gels obtained from fibrinogen/albumin mixtures (Figure 6A) have cables with an approximately uniform width and an axial modulation. In citrate-treated plasma (Figure 6B), individual fibers appear to intertwine into loose bundles (Buchanan et al., 1977) which are sometimes visible to the naked eye. With recalcification and thrombin addition (Figure 6C), individual fibers cannot be resolved, and the cables are fine, regular in width, and without axial features. The gels obtained in Figures 3 and 4, in the presence of free calcium only, lacked distinct features but were studied only at low orientation. However, the plasma used in Figure 5 polymerized much more slowly on recalcification and is shown in Figure 6D. The results presented here suggest that the diameter of the cables of the higher order structure increases with the average fiber thickness. It whould be interesting to compare the fiber diffraction patterns from oriented fibrin prepared under these different conditions in order to find out if this polymorphism is present at a more detailed structural level.

The experiments reported here demonstrate that magnetic orientation can be employed to study the joint properties of assembly and structure over a wide range of conditions. Clot formation can also be followed in platelet-rich plasma but not in whole blood as light scattering is prohibitive. It might also be possible to study fibrinolysis by monitoring the decay in birefringence of oriented clots. Very strong magnetic fields are not a prerequisite (Figure 3). Light scattering has been most successful in elucidating the pregelation phase of assembly in purified systems (Hantgan & Hermans, 1979). Magnetic birefringence gives complementary information in the postgelation phase and can be used with equal facility to study simple or complex systems.

ACKNOWLEDGMENTS

I am indebted to J.-M. Freyssinet and G. Maret, who respectively helped with sample preparation and birefringence measurements. I thank H. Dresler for technical assistance and Y. Fournet and D. Lehmann for collecting blood samples. I am also grateful to J. Hudry-Clergeon and S. J. Edelstein for commenting on the manuscript. I also thank the Service National des Champs Intenses.

Registry No. Thrombin, 9002-04-4; Ca, 7440-70-2.

REFERENCES

Buchanan, J. M., Chen, L. B., Hamazaki, T., Lenk, E., & Waugh, D. F. (1977) in *Chemistry and Biology of Thrombin* (Lundblad, R. L., Fenton, J. W., & Mann, K. G., Eds.) pp 263–273, Ann Arbor Science Publishers, Stoneham, MA.

Chen, A. B., Amrani, D. L., & Mosesson, M. W. (1977) *Biochim. Biophys. Acta 493*, 310–322.

Dhall, T. Z., Shah, G. A., Ferguson, I. A., & Dhall, D. P. (1983) *Thromb. Haemostasis 49*, 42–46.

Doolittle, R. F. (1984) *Annu. Rev. Biochem. 53*, 195–229.
Engvall, E., & Ruoslahti, E. (1977) *Int. J. Cancer 20*, 1–5.
Folk, J. E., & Finlayson, J. S. (1977) *Adv. Protein Chem. 31*, 1–133.
Freyssinet, J. M., Torbet, J., Hudry-Clergeon, G., & Maret, G. (1983) *Proc. Natl. Acad. Sci. U.S.A. 80*, 1616–1620.
Furie, B. C., & Furie, B. (1976) *Methods Enzymol. 45*, 191–205.
Ganguly, P., Chelladurai, M., Fossett, N., & Jefferson, W. (1983) *Biochem. Biophys. Res. Commun. 116*, 189–194.
Garman, A. J., & Smith, R. A. G. (1982) *Thromb. Res. 27*, 311–320.
Gormsen, J., Fletcher, A. P., Alkjaersing, N., & Sherry, S. (1967) *Arch. Biochem. Biophys. 120*, 654–665.
Greenberg, C. S., & Shuman, M. A. (1982) *J. Biol. Chem. 257*, 6096–6101.
Hantgan, R. R., & Hermans, J. (1979) *J. Biol. Chem. 254*, 11272–11281.
Hermans, J., & McDonagh, J. (1982) *Semin. Thromb. Hemostasis 8*, 11–24.
Hewat, E. A., Tranqui, L., & Wade, R. H. (1983) *J. Mol. Biol. 170*, 203–222.
Jackson, C. M., & Nemerson, Y. (1980) *Annu. Rev. Biochem. 49*, 765–811.
Janus, T. J., Lewis, S. D., Lorand, L., & Shafer, J. A. (1983) *Biochemistry 22*, 6269–6272.
Kekwick, R. A., Mackay, M. E., Nance, M. M., & Record, B. H. (1955) *Biochem. J. 60*, 671–683.
Lorand, L., & Jacobsen, A. (1962) *Nature (London) 195*, 911–912.
Maret, G., & Weill, G. (1983) *Biopolymers 22*, 2727–2744.
Messmore, H. L. (1982) *Semin. Thromb. Hemostasis 8*, 267–275.
Minton, A. P. (1981) *Biopolymers 20*, 2093–2120.
Minton, A. P. (1983) *Mol. Cell. Biochem. 55*, 119–140.
Mosher, D. F. (1976) *J. Biol. Chem. 251*, 1639–1645.
Müller, M. F., Ris, H., & Ferry, J. D. (1984) *J. Mol. Biol. 174*, 369–384.
Nemerson, Y., & Furie, B. (1980) *CRC Crit. Rev. Biochem. 9*, 45–85.
Rakoczi, I., Wiman, B., & Collen, D. (1978) *Biochim. Biophys. Acta 540*, 295–300.
Sakata, Y., & Aoki, N. (1980) *J. Clin. Invest. 65*, 290–297.
Sakata, Y., Mimuro, J., & Aoki, N. (1984) *Blood 63*, 1393–1401.
Shah, G. A., Ferguson, I. A., Dhall, T. Z., & Dhall, D. P. (1982) *Biopolymers 21*, 1037–1047.
Tamaki, T., & Aoki, N. (1981) *Biochim. Biophys. Acta 661*, 280–286.
Torbet, J. (1986) *Biophysical Uses of Steady Magnetic Fields* (Maret, G., Kiepenheuer, J., & Boccara, N., Eds.) Springer-Verlag, New York and Berlin.
Torbet, J., Freyssinet, J. M., & Hudry-Clergeon, G. (1981) *Nature (London) 289*, 91–93.
Wilf, J., Gladner, J. A., & Minton, A. P. (1985) *Thromb. Res. 37*, 681–688.

Crystal Structure of Substrate-Free *Pseudomonas putida* Cytochrome P-450†

Thomas L. Poulos,* Barry C. Finzel, and Andrew J. Howard
Protein Engineering Department, Genex Corporation, 16020 Industrial Drive, Gaithersburg, Maryland 20877
Received February 27, 1986; Revised Manuscript Received April 30, 1986

ABSTRACT: The crystal structure of *Pseudomonas putida* cytochrome P-450$_{cam}$ in the substrate-free form has been refined at 2.20-Å resolution and compared to the substrate-bound form of the enzyme. In the absence of the substrate camphor, the P-450$_{cam}$ heme iron atom is hexacoordinate with the sulfur atom of Cys-357 providing one axial heme ligand and a water molecule or hydroxide ion providing the other axial ligand. A network of hydrogen-bonded solvent molecules occupies the substrate pocket in addition to the iron-linked aqua ligand. When a camphor molecule binds, the active site waters including the aqua ligand are displaced, resulting in a pentacoordinate high-spin heme iron atom. Analysis of the $F_{\text{no camphor}} - F_{\text{camphor}}$ difference Fourier and a quantitative comparison of the two refined structures reveal that no detectable conformational change results from camphor binding other than a small repositioning of a phenylalanine side chain that contacts the camphor molecule. However, large decreases in the mean temperature factors of three separate segments of the protein centered on Tyr-96, Thr-185, and Asp-251 result from camphor binding. This indicates that camphor binding decreases the flexibility in these three regions of the P-450$_{cam}$ molecule without altering the mean position of the atoms involved.

Cytochromes P-450 are a group of *b*-type heme proteins that catalyze the hydroxylation of aromatic or aliphatic substrates in a variety of metabolic processes of both prokaryotes and eukaryotes. While a large number of P-450s have been purified and characterized, the cytochrome P-450 camphor 5-exohydroxylase (P-450$_{cam}$) from the soil bacterium *Pseudomonas putida* has provided the most detailed structural and mechanistic information on P-450 monooxygenases (Wagner & Gunsalus, 1982; Gunsalus et al., 1980; Debrunner et al., 1978; Gunsalus & Sligar, 1978).

P-450$_{cam}$ is a 45 000-dalton polypeptide chain containing a single ferric protoporphyrin IX. An abbreviated catalytic cycle for P-450$_{cam}$ is depicted in Scheme I. As in other *b*-type heme proteins, the ferric (Fe^{3+}) iron atom in P-450$_{cam}$ equilibrates between the low-spin state, $S = {}^1/_2$, and the high-spin state, $S = {}^5/_2$ (Sharrock et al., 1976; Tsai et al., 1970). As depicted in Scheme I, the low-spin state is favored in the absence of substrate, and the iron atom is hexacoordinate with X representing an unidentified axial ligand. In the presence of

† This work was supported in part by NIH Grants GM 33325 and GM 33688.

0006-2960/86/0425-5314$01.50/0